ISSN No:-2456-2165

Leaching of Coal Fly Ash by Sulphuric Acid for the Synthesis of Wastewater Treatment Polymeric Coagulant

M. Clotilde Apua
School of Chemical and Metallurgical Engineering,
University of the Witwatersrand,
Johannesburg, South Africa

Abstract:- Coal fly ash (CFA) sample produced in coal-burning power plants contains significant quantities of oxides of aluminium, iron and other important elements such as magnesium, silicon and calcium for the production of coagulant for wastewater treatment. In order to synthesize a coagulant, the dissolution of these CFA elements was studied in sulphuric acid (H_2SO_4) solutions. The impacts of dissolution time, H_2SO_4 concentration, temperature and solid/liquid ratio were investigated for the leaching process. The treated CFA samples were characterized by PSD, XRD, XRF, FTIR and SEM. Thermodynamic feasibility was studied using Hydra/Medusa software. The dissolution efficiencies of aluminium, iron, magnesium, silicon and calcium were 33.86, 57.90, 73.21, 11.12 and 25.43%, respectively, in 1.5 M H_2SO_4, with a pH ranging from 0.5 to 3.9, at 300 rpm, 150 °C, a solid/liquid ratio of 0.20 and a leaching time of 6 hours. The PSD results revealed that particle size changes happened during the leaching process, XRD and FTIR showed the presence of the same mineral phases in the raw and treated CFA samples, and SEM indicated that both a porous structure and a stem-like structure were formed after leaching. The generated dissolution solution containing polymeric sulphates of aluminium, iron, magnesium, silicon and calcium can be utilized as coagulant in the treatment of wastewater. The process can be easily adopted to synthesize complex coagulant, therefore decreasing CFA pollution and producing a valuable coagulant.

Keywords:- *Synthesis; Pressure sulphuric acid-leaching; Coal fly ash; Coagulant; Wastewater.*

I. INTRODUCTION

Energy production from coal combustion at 1200–1700 °C generates considerable by-products that create serious storage and/or disposal management issues [1]. These by-products consist of bottom ash, fly ash and slag. These waste by-products are normally dumped and/or disposed of, but therefore pollute the environment. Due to the limited commercial uses of coal fly ash (CFA), in particular, extensive research has been conducted to discover some alternative uses [2,3].

At present, research has shown that only a small part of the total CFA production (20–30%) is utilized in the following applications: synthesis of geopolymers [4,5], asphalt filler [3], production of zeolites [6], substitute material for cement [7], adsorbent of single contaminants in flue gases [8–10], flowable fill [11], manufacture of ceramics and glass [12,13], soil stabilization [14,15], catalysts and catalyst supports [16,17], wastewater treatments as an adsorbent for organic removal [18,19], and extraction of metals [20,21].

However, despite the various uses listed above, there is still a need to discover other means of using CFA productively in order to protect the environment and to reduce its disposal on land [22]. Currently, CFA has promising uses in wastewater treatment due to its physical properties such as surface area and porosity, and the presence of chemical components such as aluminium and iron oxides. The main chemical components of CFA are aluminium, iron, calcium, silicon and magnesium oxides. Iron and aluminium oxides are important raw materials for the production of coagulants for the treatment of wastewater through the coagulation process. It is notable that over the years, most coagulant companies have used ores or chemical salts of aluminium and iron as raw materials. Nevertheless, aluminium and iron minerals or chemical salts of iron and aluminium are expensive [23]. Moreover, several researchers have studied the role of other elements, such us silicon, magnesium and calcium ions, as potential coagulants for wastewater treatment [24–26]. Coal fly ash also contains several other strategic elements, some of which (silicon, magnesium and calcium) could be extracted together with aluminium and iron. Thus, CFA has become an important resource for the synthesis of coagulants and researchers are more interested in this study currently [2]. Therefore, the use of CFA to make composite (polymeric) coagulants can provide significant cost savings, as CFA is much cheaper than industrial grade iron or aluminium ores. In addition, such a concept of using these by-products would reduce the environmental degradation resulting from storage and disposal techniques currently used in several countries [23].

Therefore, the aim of this research was to use CFA, a known source of solid waste currently increasing worldwide, which is available in South Africa, as synthesis raw material to produce a polymeric coagulant for wastewater treatment. This paper presents a process for the synthesis of a composite coagulant by direct pressure leaching of aluminium, iron and other strategic elements from CFA in H_2SO_4 solution. The study on the performance of the synthesized CFA-based coagulant in wastewater treatment is discussed elsewhere [27].

ISSN No:-2456-2165

II. EXPERIMENTAL

A. *Sample characterization*

The CFA sample collected from the electrostatic precipitators at the Kendal power station located in Mpumalanga province, South Africa. High purity H_2SO_4 was used for the dissolution tests. The particle size distribution (PSD) was measured by a Microtrac S3500 laser-based particle size analyser and the results are displayed in Fig. 1. PSD with a P80 particle diameter of 49 µm was found. Mineralogical analysis was carried out using a Rigaku Ultima IV Model X-ray diffractometer (XRD) and the pattern is shown in Fig. 2. The major crystalline phases present in the sample are quartz (SiO_2), hematite (Fe_2O_3), and mullite ($Al_{5.65}Si_{0.35}O_{9.175}$). The elemental analysis of the CFA was carried out using a Rigaku ZSX Primus II X-ray fluorescence (XRF) apparatus and the results are given in Table 1. It is shown that the CFA contains Fe_2O_3 (4.16%), Al_2O_3 (32.15%), SiO_2 (49.92%). CaO (6.25%), and MgO (1.40%). The morphology of the CFA presented in Fig. 3 was performed using a TESCAN scanning electron microscope (SEM) and it was observed that CFA particles have smooth spherical surfaces. While the CFA pattern was performed using a Thermo Scientific Nicolet iS10 spectrometer (wavenumber region of 500–4000 cm^{-1}) and the results are shown in Fig. 4 which reveals the presence of Si–O, Al–O, P=O, and O–H groups in the sample.

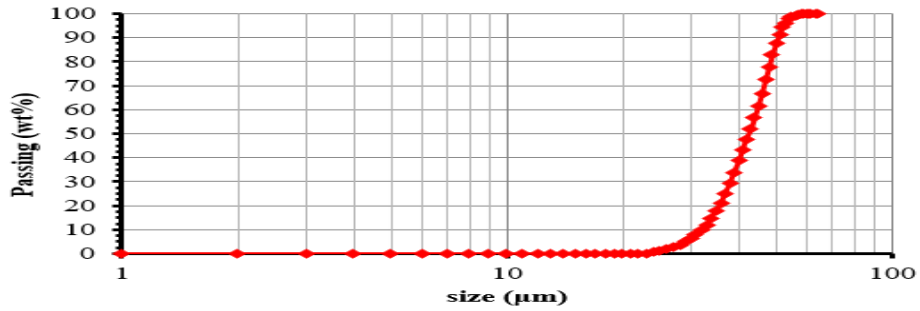

Fig. 1: Curve of particle size distribution of coal fly ash sample.

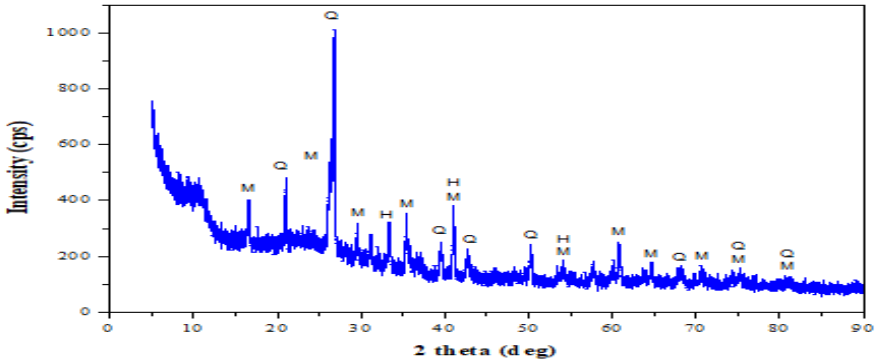

Fig. 2: XRD pattern of coal fly ash. Q, M, and H indicate quartz (SiO_2), mullite ($Al_{5.65}Si_{0.35}O_{9.175}$), and hematite ($Fe_2O_3$), respectively

Chemical composition	Al_2O_3	Fe_2O_3	SiO_2	CaO	TiO_2	MgO	K_2O	P_2O_5
Content (wt%)	32.15	4.16	49.92	6.25	2.15	1.4	1	1.04

Table 1: Chemical composition of coal ash sample

Only important elements from important phases are presented.

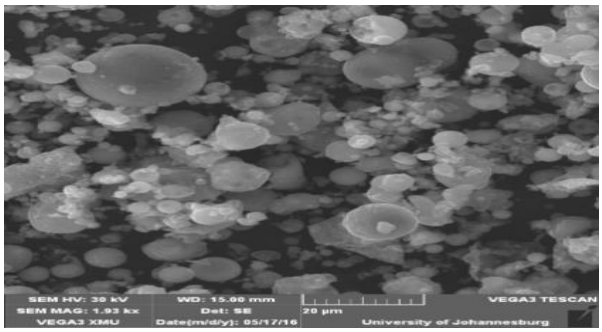

Fig. 3: SEM of the coal fly ash showing smooth spheres

ISSN No:-2456-2165

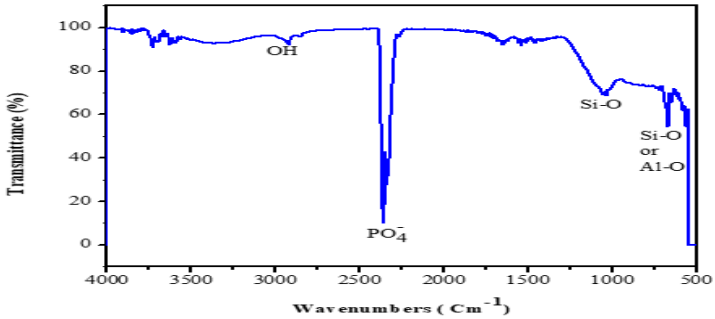

Fig. 4: FTIR spectrum for coal fly ash

B. Coagulant synthesis

Dissolution process was conducted in a 750 mL high pressure reactor. 40 g of CFA and required amounts of H_2SO_4 solution were used for the leaching, while the stirring of the slurry was performed using of a magnetic stirrer. Dissolution parameters such as H_2SO_4 concentration from 0.5 to 6.0 M, temperature range of 25 to 190 °C, solid/liquid (S/L) ratio from 0.17 to 0.40, and leaching time from 1 to 6 hours, were investigated to obtain optimal experimental conditions. For the effect of temperature, the reaction begins when the temperature reaches the selected value. A sample of the leach residue was washed three times with deionized water, oven dried at 50 °C overnight, re-ground and analyzed by PSD, XRD, XRF, FTIR and SEM. Leaching recoveries of iron, aluminium, silicon, magnesium and calcium were calculated, respectively, in relation to the percentages of iron, aluminium, silicon, magnesium and calcium in the CFA sample.

III. RESULTS AND DISCUSSION

Batch dissolution tests were carried out for each selected parameter to study the leaching behaviour of iron, aluminium, and other elements from CFA material. The dissolution solution used for the leaching of elements from CFA sample was an aqueous solution of H_2SO_4. A sample of CFA containing 17.01% aluminium and 2.91% iron was used. In general, iron and aluminium in CFA are found together with other elements such as magnesium, silicon, calcium, titanium and potassium. Among these elements, the dissolutions of silicon, calcium and magnesium were investigated.

In this study, aluminium and iron in the CFA sample had to be leached with H_2SO_4 to produce their soluble forms. In order to predict the predominance areas of different aluminium and iron species in an aqueous solution, Eh-pH diagrams for the Fe–SO_4^{2-}–H_2O system and Al–SO_4^{2-}–H_2O system at 25 °C (for a solution of total sulphate concentration = 1.5 M) were drawn using the Hydra/Medusa software and presented in Fig. 5. The total sulphate concentrations of 1.5 M were chosen according to diluted H_2SO_4 solutions. It is noticed from Fig. 5(a) that for a 1.5 M total sulphate concentration solution, Fe^{3+} (i.e. $FeSO_4^{2-}$ complex) is the most predominant species at pH below 3.9 and Eh between 0.67 and 1.00 V; hydrolysis of $Fe(SO_4)_2^-$ occurs with increasing pH forming species such FeS_2, Fe_2O_3, and $Fe(HS)_3$ which are predominant species at pH values above 4. Fig. 5(b) shows that leached aluminium species Al^{3+}, $AlSO_4^+$ and $Al(SO_4)^{2-}$ are stable in the pH region below 5 and the Eh range of -1.00 to 1.00 V. Therefore, dissolution parameters selected from the chemical equilibrium diagrams in Fig. 5 were: pH 0.5 to 3.9.

Generally, aqueous equilibrium reactions of iron and aluminium in H_2SO_4 media are given in (1) – (6) [28–30]. In aqueous H_2SO_4 solutions given in (6), iron distributes as Fe(II) and Fe(III) soluble species such as free ions (Fe^{2+} and Fe^{3+}) or complex compounds [$FeSO_4^0$, $FeSO_4^+$, $Fe(SO_4)_2^-$] as illustrated in (1) – (3) [31,32]. Aluminium, on the other hand, goes into solution as Al (III) species such as simple cations (Al^{3+}) or charged complexes [$AlSO_4^+$, $Al(SO_4)_2^-$] as presented in (4) and (5) [33]. The concentrations of iron and aluminium are highly dependent on the initial total amount of iron, aluminium, acidity and temperature [32].

$$Fe^{2+} + SO_4^{2-} \leftrightarrow FeSO_4^0 \quad (1)$$

$$Fe^{3+} + SO_4^{2-} \leftrightarrow FeSO_4^+ \quad (2)$$

$$Fe^{3+} + 2SO_4^{2-} \leftrightarrow Fe(SO_4)_2^- \quad (3)$$

$$Al^{3+} + SO_4^{2-} \leftrightarrow AlSO_4^+ \quad (4)$$

$$Al^{3+} + 2SO_4^{2-} \leftrightarrow Al(SO_4)_2^- \quad (5)$$

$$H^+ + SO_4^{2-} \leftrightarrow HSO_4^- \quad (6)$$

Chemistry of H_2SO_4 leaching of iron and aluminium from Fe_2O_3 and Al_2O_3 in coal fly ash

The aim was to leach iron and aluminium from Fe_2O_3 and Al_2O_3, respectively, in the CFA sample with H_2SO_4 solutions. Throughout the leaching of iron and aluminium with H_2SO_4, the mechanism that describes complexation of iron and aluminium is given by (2) – (6). The overall reactions are illustrated in (7) and (8) for iron and aluminium, respectively [34].

$$Fe_2O_3 + 3H_2SO_4 \leftrightarrow Fe_2(SO_4)_3 + 3H_2O \quad (7)$$

$$Al_2O_3 + 3H_2SO_4 \leftrightarrow Al_2(SO_4)_3 + 3H_2O \quad (8)$$

H_2SO_4 reacts with iron and aluminium in CFA to, respectively, produce $FeSO_4^+$ and $AlSO_4^+$ complexes on the surface of iron and aluminium metals as illustrated in (2) and (4). Subsequently, $FeSO_4^+$ undergoes another complexation with the sulphate ion to produce $Fe(SO_4)_2^-$ (3) which passes in solution while $AlSO_4^+$ enters in complexation with sulphate ion to form $Al(SO_4)_2^-$ which goes into solution (5). Theoretically, the dissolution of iron and aluminium occurs as presented in (2) – (6) at pH < 3.9. Moreover, the effects of

ISSN No:-2456-2165

reaction parameters on the dissolution of elements in CFA are investigated in order to optimize the process.

A. Effect of time

The impact of time on the dissolution of iron, aluminium and other CFA elements at room temperature (RT = 23±2 °C), was studied in the range of 1 to 6 hours. The results are presented in Fig. 6. It was mainly noticed that the leaching of iron, aluminium, silicon and magnesium at the concentration of 1 M H_2SO_4 at RT is completed within 1 hour. It is found that extraction efficiencies of iron, aluminium, silicon and magnesium after 1 hour of leaching at RT reached 7.97, 10.25, 10.21 and 60.15%, respectively, with no calcium reported after 6 hours. Practically, 1 hour of dissolution was found to be optimum.

B. Effect of H_2SO_4 concentration

The effect of H_2SO_4 concentration on the leaching of iron, aluminium, silicon, magnesium and calcium at RT was studied in the range of 0.5 to 6.0 M H_2SO_4. The results are presented in Fig. 7. When the concentration of H_2SO_4 was below 1.5 M, it can be seen that the recovery gradually increases for iron from 10.83% to 14.96% and for aluminium from 14.08% to 16.00% with the H_2SO_4 concentration at RT. Thereafter, with a H_2SO_4 concentration of 1.5 M, the recoveries of iron and aluminium reach a plateau. Mainly, it was observed in Fig. 7 that the dissolution of iron, as well as the leaching of aluminium, is completed when 1.5 M H_2SO_4 was used. Within the whole concentration range of H_2SO_4, magnesium and silicon are also dissolved with iron and aluminium. Maximum recoveries of 42.32 and 11.52% were obtained for magnesium and silicon, respectively. No calcium was detected in the leach solution under these conditions.

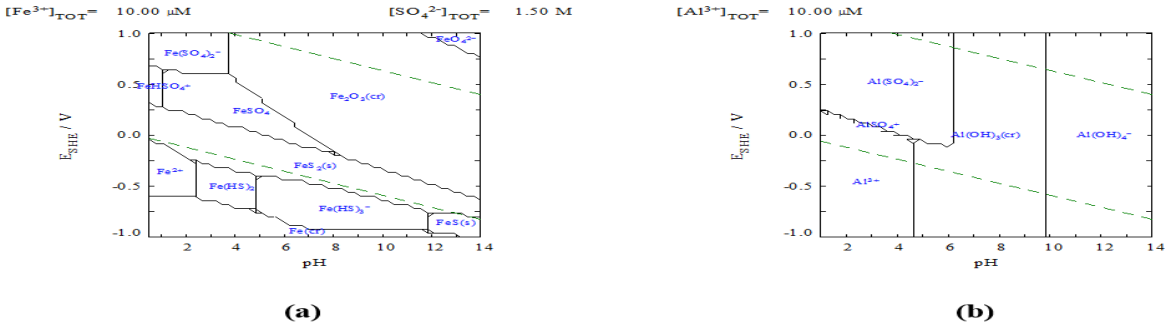

Fig. 5: Eh–pH diagram for the (a) Fe–SO_4^{2-}–H_2O system and (b) Al–SO_4^{2-}–H_2O system at 25 °C; Total SO_4^{2-} concentration = 1.5 M. These diagrams have been drawn using the Hydra/Medusa software.

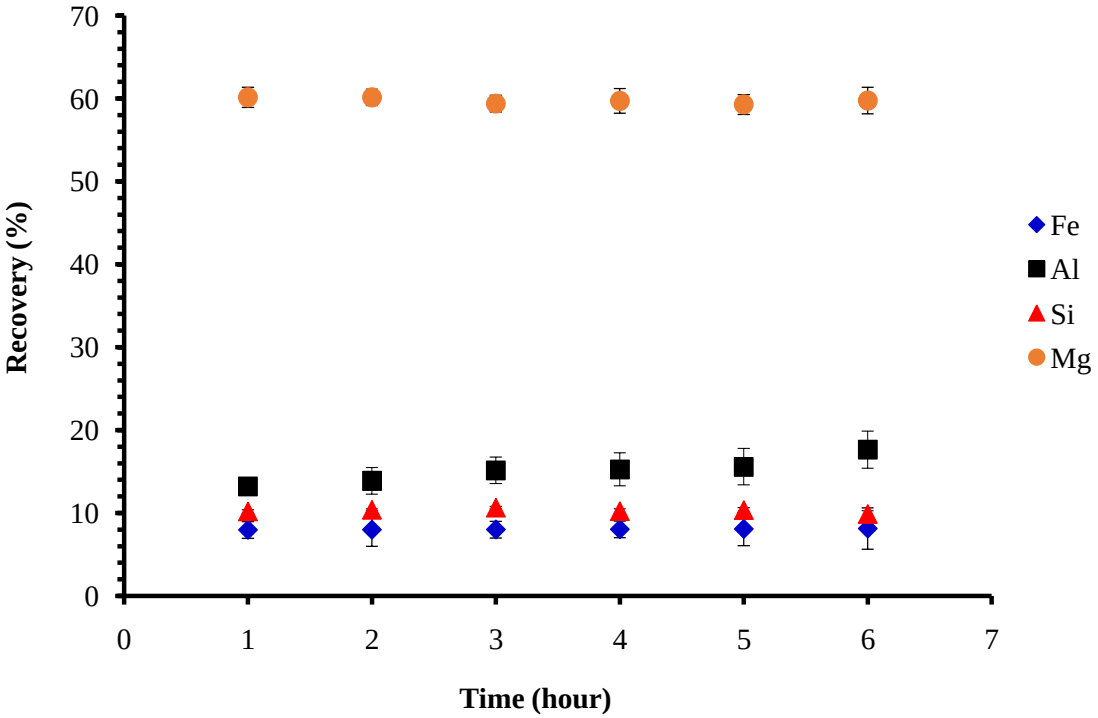

Fig. 6: Effect of time on the leaching of elements from CFA sample (particle size: −49 µm, RT (23±2 °C), 1 M H_2SO_4, 300 rpm, S/L = 0.33).

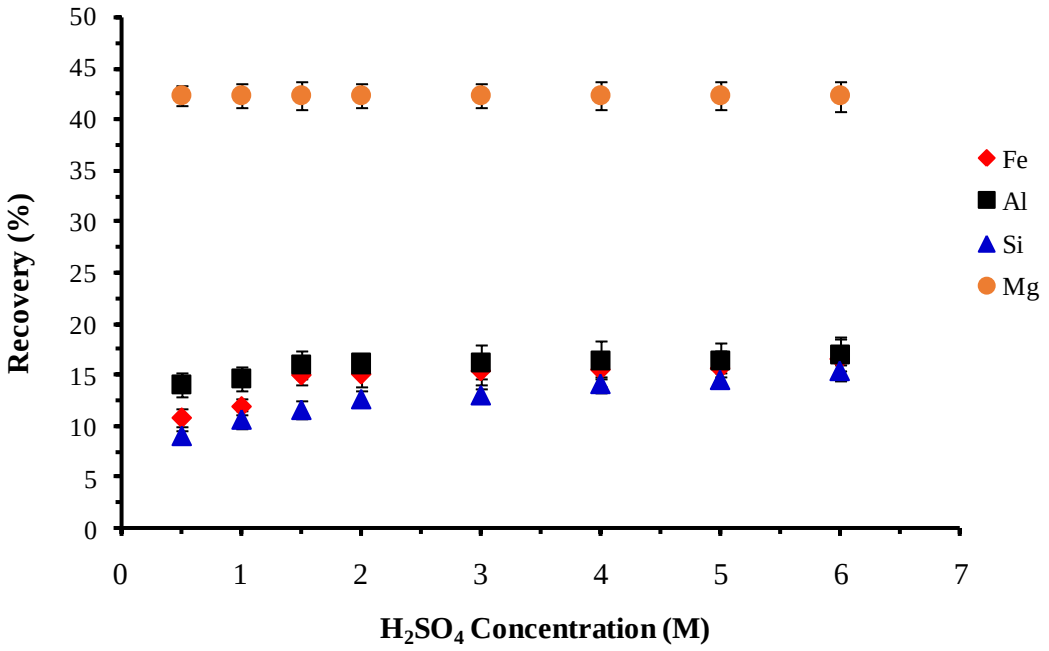

Fig. 7: Effect of H_2SO_4 concentration on the leaching of elements from CFA sample (particle size: −49 µm, RT (23±2 °C), 300 rpm, S/L= 0.33, 1 hour)

C. Effect of temperature

Fig. 8 displays the impact of temperature on the extraction efficiencies of iron, aluminium, silicon, magnesium and calcium. The major variation in extraction efficiency with temperature change is observed for iron. The CFA sample showed a highly variable leaching behaviour of elements at different temperatures. When dissolution was performed at RT, leaching of iron, aluminium, silicon and magnesium was slower. The extraction efficiency of iron increased significantly with increasing temperature from 120 °C to 190 °C, but there was no significant increase at lower temperatures. For aluminium, from 90 °C, the concentration in solution is 10.72%. There is no obvious change in the aluminium leaching as the temperature increases from 90 to 150 °C. Thereafter, the leaching decreases until the temperature reaches 190 °C. The fused structure of aluminosilicate is probably the reason for the relatively low extraction efficiency of aluminium. A similar behaviour was also observed by other researchers [35,36]. A temperature of 150 °C was considered optimal for aluminium leaching. A gradual increase in extraction efficiencies was noticed for magnesium, calcium and silicon. Maximum extraction efficiencies of 68.57, 26.09 and 22.07% were obtained for magnesium, calcium and silicon, respectively.

D. Effect of solid/liquid ratio

Fig. 9 indicates that the S/L ratio has a substantial effect on the leaching of iron and magnesium than on the leaching of other elements with H_2SO_4. The concentration of iron in the leaching solution (composite coagulant) increased with increasing S/L ratio from 0.17 to 0.20, then significantly decreased with further increases in S/L ratio. This can be justified by the fact that high S/L ratio leads to a starvation of reagent. For example, it was found that with an S/L ratio of 0.20, more than 90% of the iron was extracted. A similar trend was noticed in the dissolutions of aluminium and other elements (silicon, magnesium and calcium) for different S/L ratios under identical conditions. Maximum extraction efficiencies of 28.88, 7.81, 78.67, and 27.11% were obtained for aluminium, silicon, magnesium and calcium respectively at a S/L ratio of 0.20. In comparison to the dissolution behaviour of iron, the low dissolution efficiencies of aluminium and silicon (<30%) are probably due to the structure and property of aluminium and silicon oxides in CFA. The mineralogy of CFA is extremely diverse. The identified phase of iron oxide is hematite which can be easily leached in H_2SO_4 solution [3]. In CFA, the Al_2O_3 is found either as crystalline mullite form and non-crystalline amorphous form or bound to an aluminosilicate glass matrix [3,37]. The glass matrix and mullite phase are not easily accessible to direct acid dissolution [36].

E. Effect of time on optimal experimental conditions

The effect of time on optimal experimental conditions was investigated and results are presented in Fig.10. Magnesium dissolved faster than iron and aluminium, while silicon and calcium showed a surprising difference in dissolution behaviour. The concentrations of iron, aluminium, silicon, magnesium and calcium in the composite coagulant solution increased with time up to 57.90, 33.86, 11.12, 73.21 and 25.43% respectively for 6 hours. It is shown that below 3 hours of dissolution time, the concentration of iron decreased dramatically in the produced complex coagulant solution. This can be explained by the dissolution and precipitation of iron, which can be associated with many factors such as temperature, solution concentration, and the presence of some ions in the environment. It is reported that depending on solution concentration and temperature, a large number of iron

ISSN No:-2456-2165

minerals in aqueous H_2SO_4 solutions could precipitate, such as hydrous ferric oxides (Fe_2O_3 nH_2O) and hydronium jarosite [$H_3OFe_3(SO_4)_2(OH)_6$] [31,38]. This point is further confirmed by the results from XRD analysis of the treated CFA (Fig. 12). After 3 hours, the self - inhibition effect of iron to the mass transfer is influenced by the dissolution of other ions from the solid site. The extraction efficiency of iron then increased. The lower leaching of aluminium may be due the presence of an unfavourable structure of aluminium oxides, resulting from the combustion of coal at high temperatures. Low silicon leaching is common in an acidic environment and may be due to the mineral structure of CFA which favours an alkaline solution to leach silicon [39].

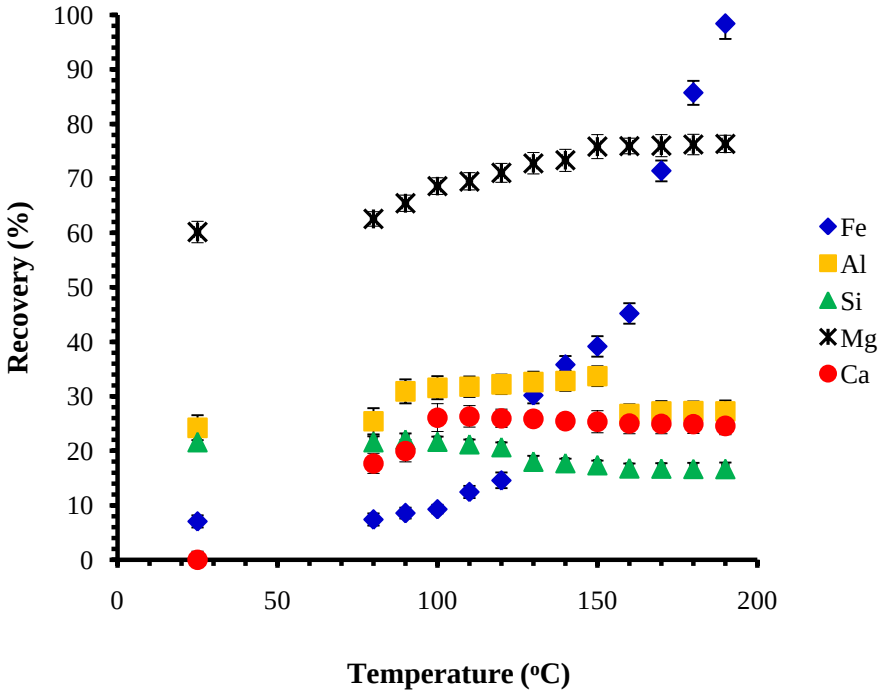

Fig. 8: Effect of temperature on the leaching of elements from CFA sample (particle size: −49 µm, 1.5 M H_2SO_4, 300 rpm, S/L= 0.33, 1 hour).

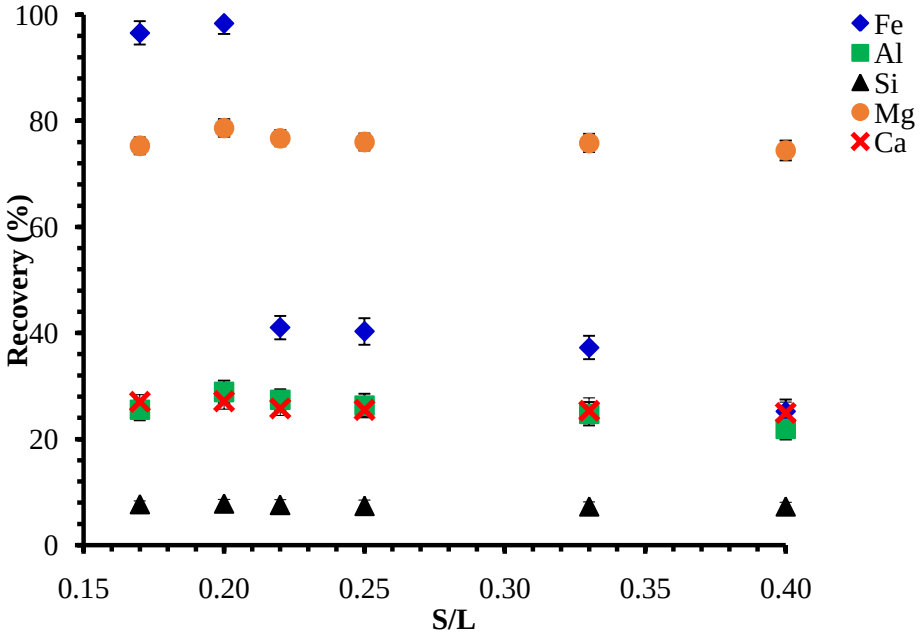

Fig. 9: Effect of S/L ratio on the leaching of elements from CFA sample (particle size: −49 µm, 1.5 M H_2SO_4, 150°C, 300 rpm, 1 hour).

ISSN No:-2456-2165

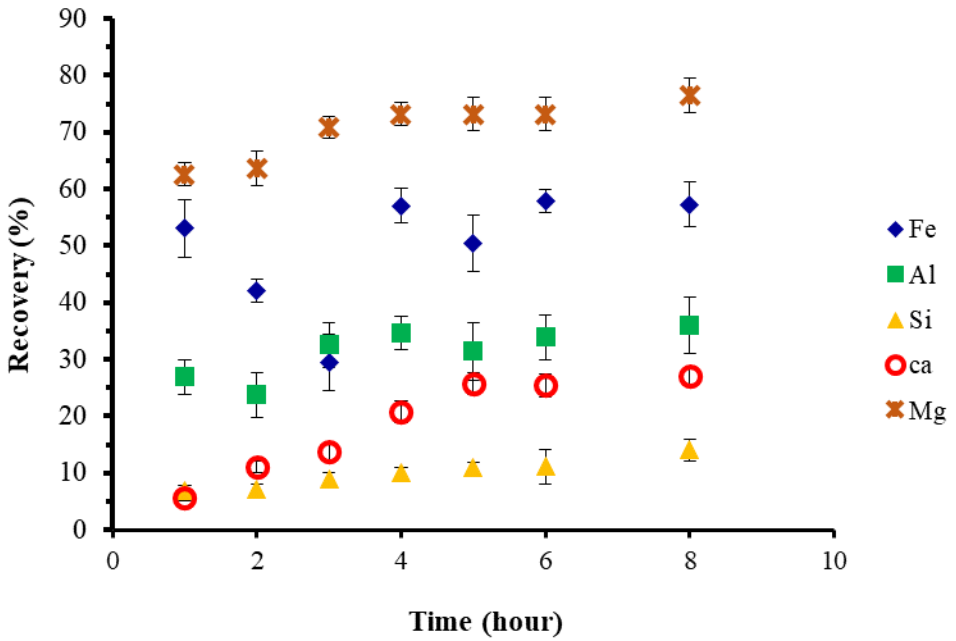

Fig. 10: Effect of time on optimal experimental conditions
(particle size: −49 µm, 1.5 M H_2SO_4, 150 °C, S/L= 0.20, 300 rpm)

F. Characteristics of the synthesized coagulant solution

The complex coagulant produced from the leaching of CFA was a dark green colour liquid. Chemical properties of the coagulant (synthesized under optimal experimental conditions at 150 °C for 6 hours) are reported in Table 2. Moreover, in a study by [27], the synthesized CFA-based complex coagulant was found to be effective in removing impurities from acid mine drainage.

Properties of the synthesized complex coagulant at 150 °C for 6 h	
pH	0.68–0.75 (< 4)
Colour	dark green
Fe	21731.89 mg/L
Al	603.18 mg/L
Si	96.00 mg/L
Mg	1366.70 mg/L
Ca	mg/L

Table 2: Chemical composition of the synthesized coagulant.

G. Analysis of the treated coal fly ash

Treated CFA samples from the optimal experimental conditions were analysed by PSD, XRD, XRF, FTIR and SEM in order to compare them with the raw CFA and measure the impact of H_2SO_4 leaching.

a) PSD analysis

Comparison of the PSD results in Figs. 11 and 1 showed that changes in particle size occurred during the dissolution process as average particle sizes at 80% weight of 47 µm and 49 µm were determined for the treated and raw CFA samples, respectively.

b) XRD and XRF analyses

It is observed from the XRD pattern in Fig. 12 that the characteristics of the mineral matter in the raw CFA sample were revealed in the treated CFA. However, throughout reaction with varying times secondary mineral phases such as jarosite ($2Fe_3(OH)_6(SO_4)_2$), and gypsum ($CaSO_4.2H_2O$) were formed. It is established that the formation of jarosite is based on the presence of iron in sulphate medium and the tendency of iron sulphate to hydrolyze at pH less than 3 and at temperatures between 20 and 200 °C [41,42]. Therefore, in H_2SO_4 environment containing CFA, jarosite precipitate can be formed according to reaction in (9) [41,42]. The XRD results of the treated CFA are in agreement with the results in Fig. 10. Furthermore, the formation of gypsum is based on the presence of calcium in H_2SO_4 aqueous solution in which CaO (in CFA) tends to dissolve in water to produce $Ca(OH)_2$ which will react with H_2SO_4 as per (10) [43].

$$3Fe_2(SO_4)_3 + X_2SO_4 + 12H_2O \rightarrow 2Fe_3X(OH)_6(SO_4)_2\downarrow + 6H_2SO_4 \quad (9)$$

Where X is the hydronium ion.

$$Ca(OH)_2 + 2H^+ + SO_4^{2-} + 2H_2O \rightarrow CaSO_4.2H_2O\downarrow + 2H^+ + 2OH^- \quad (10)$$

Table 3 shows that there is not much change in the XRF results of the raw and the treated CFA samples. These results are consistent with XRD results (in Fig. 12).

ISSN No:-2456-2165

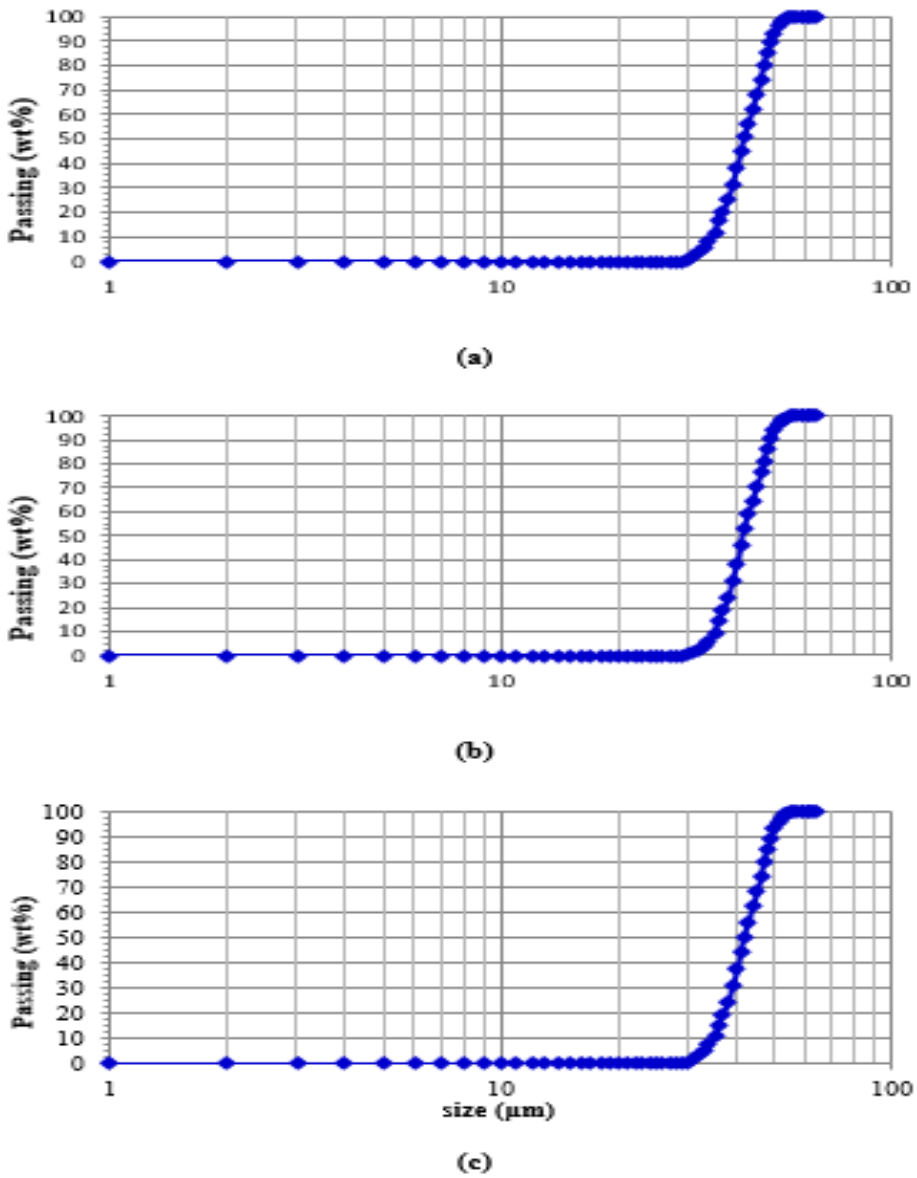

Fig. 11: PSD of the treated CFA with H_2SO_4 under optimal experimental conditions at different leaching stages: (a) 1 hour leaching, (b) 3 hours leaching, and (c) 6 hours leaching.

Chemical composition	Content (wt%)							
	Raw CFA	Treated CFA						
		1 h	2 h	3 h	4 h	5 h	6 h	8 h
Al_2O_3	32.15	28.20	26.50	24.10	25.20	25.20	25.60	25.96
Fe_2O_3	4.16	2.34	2.60	3.26	2.14	2.36	2.10	2.19
SiO_2	49.92	49.50	49.40	49.30	49.26	49.10	49.50	49.22
CaO	6.25	5.59	5.03	5.18	5.95	6.17	5.60	4.81
TiO_2	2.15	2.13	2.15	2.15	2.14	2.14	2.15	2.15
MgO	1.40	0.46	0.56	0.57	0.45	0.46	0.45	0.42
K_2O	1.00	1.03	1.14	1.11	1.05	1.07	1.05	1.09
P_2O_5	1.04	0.16	0.18	0.21	0.17	0.19	0.17	0.19

Table 3: Chemical composition of the raw and treated CFA samples.
Only important elements from important phases are presented

c) FTIR analysis

ISSN No:-2456-2165

From the FTIR spectrum in Fig. 13, peaks in the wavenumber ranges from 950–1168 cm^{-1} and 550–920 cm^{-1} originated from quartz and mullite are practically unchanged after leaching, so that the identifiable chemical bonds remained practically unchanged. The same mineral phases are found in both the raw and treated CFA samples. This fact was previously established by results from XRD and XRF analyses (Fig. 12 and Table 3). Furthermore, the raw CFA shows strong absorption band at 2359 cm^{-1} for P=O bond. This suggests that reaction occurred during the leaching process.

The SEM images of the untreated and treated samples in Fig. 14 indicate the marked impact of the H_2SO_4 solution. The surface morphology of the untreated CFA particles (image a) looks relatively smooth. The morphologies of the treated CFA in images (b), (c) and (d) are almost completely uniform compare to the agglomerations of particles in the raw (image a). Images (b), (c) and (d) reveal that a porous structure was formed after leaching. In addition, the dissolution of H_2SO_4 produces a stem-like structure which indicates the formation of new phases. This fact is earlier established by results from XRD analysis (in Fig.12).

d) SEM analysis

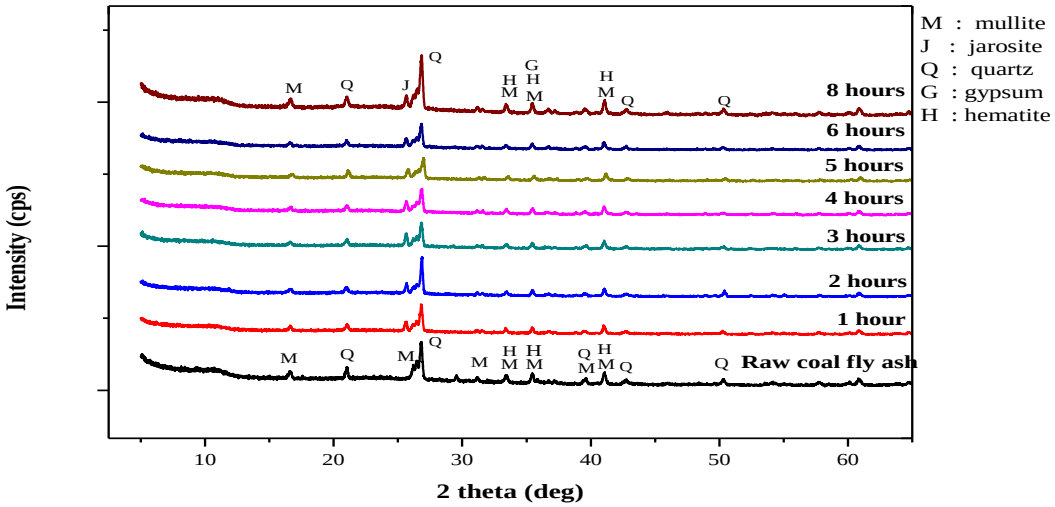

Figure 12: Comparison of XRD pattern of the raw to the treated CFA with H_2SO_4 leaching under optimal experimental conditions in different times.

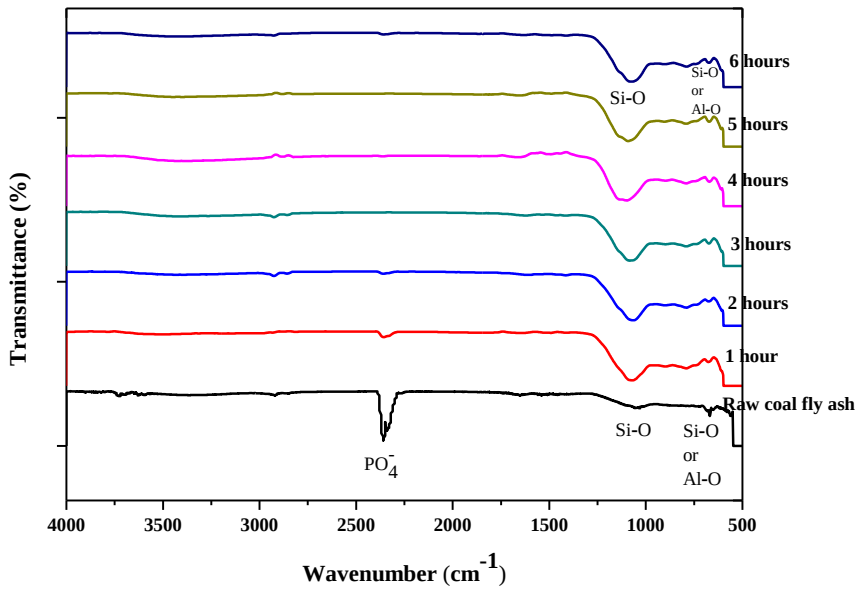

Fig. 13: Comparison of FTIR spectrum of the raw to the treated CFA by H_2SO_4 leaching under optimal experimental conditions in different times.

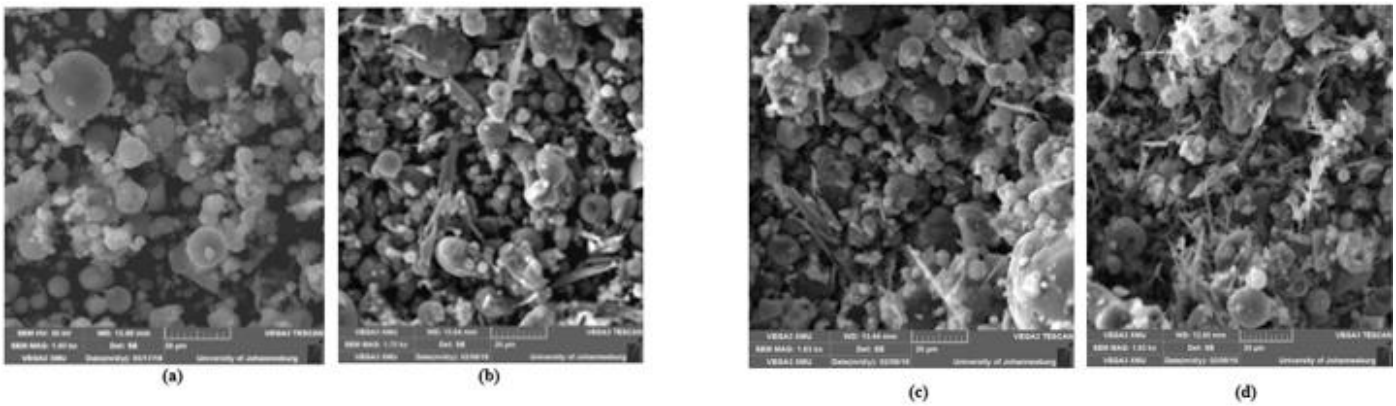

Fig. 14: SEM micrographs of CFA particles at different leaching stages. (a) raw coal fly ash; (b) coal fly ash after 1 hour leaching (c) coal fly ash after 3 hours leaching, and (d) coal fly ash after 6 hours leaching.

IV. CONCLUSION

The pressure leaching process of complex coagulant synthesis from CFA was studied. Leaching time, H_2SO_4 concentration, S/L ratio and temperature play an important role in the characteristics of the composite coagulant. Iron, aluminium, silicon, magnesium and calcium can be extracted from CFA using H_2SO_4 solution. Optimal process conditions are pH 0.3–3.9, S/L = 0.20, 1.5 M H_2SO_4 concentration, temperature = 150 °C, and time = 6 h with a stirring speed of 300 rpm using −49 µm particle size. Aluminium, calcium and silicon dissolve poorly from CFA. This may be attributed to the presence of an unfavourable structure of oxides of aluminium, calcium and silicon, resulting from the combustion of coal at high temperatures. The dissolutions of iron and magnesium increase with increasing H_2SO_4 concentration, temperature, S/L ratio, and dissolution time. The composite coagulant containing polymeric aluminium sulphate, polymeric ferric sulphate, polymeric calcium sulphate, polymeric silicon sulphate, and polymeric magnesium sulphate has been successfully produced by the reaction of CFA with H_2SO_4. The dissolution process produced a 57.90% iron, 33.86% aluminium, 11.12% silicon, 73.21% magnesium, and 25.43% calcium coagulant that can be used in wastewater treatment. The dissolution process involves change in the particle size distribution of the CFA residues. The initial average diameter of 49 µm was reduced to 47 µm during the whole dissolution phase. After the leaching process, mineral phases in the untreated CFA sample as well as new phases were identified in the treated CFA. The H_2SO_4 leaching has affected the morphology of CFA particles. Porous and stem-like structures were formed after dissolution. The process of producing such a coagulant can be adopted in wastewater treatment plants, thereby reducing the problem of CFA waste and producing a valuable chemical reagent.

V. ACKNOWLEDGEMENT

The author would like to thank Mrs Nomsa Baloyi and Mr Edward Malenga for their technical help. Gratitude is also extended to the University of Johannesburg Extraction Metallurgy Laboratory for the generous use of their equipment for assistance with PSD, SEM/EDS, XRD, XRF and FTIR.

REFERENCES

[1.] Apua, M.C., Simate, G.S. Characterization of coal fly ash for the production of coagulant for usage in wastewater treatment. *MS&T*, Curran Associates, New York. 2018, 1512–1521.
[2.] Ahmaruzzaman, M. A review on the utilization of fly ash. *Prog. Energy Combust. Sci.* 2010, 36, 327–363.
[3.] Blissett, R.S., Rowson, N.A. A review of the multi-component utilisation of coal fly ash. *Fuel*. 2012, 97, 1–23.
[4.] Barbosa, V.F.F., MacKenzie, K.J.D. Thermal behaviour of inorganic geopolymers and composites derived from sodium polysialate. *Mater. Res. Bull.* 2003, 38, 319–331.
[5.] Panias, D., Giannopoulou, I.P., Perraki, T. Effect of synthesis parameters on the mechanical properties of fly ash-based geopolymers. *Colloids and Surfaces A: Physicochem. Eng. Aspects*. 2007, 301, 246–254.
[6.] Querol, X., Moreno, N., Umana, J.C., Alastuey, A., Hernandez, E., Lopez-Soler, A., Plana, F. Synthesis of zeolites from coal fly ash: an overview. *Int. J. Coal Geol.* 2002, 50, 413–423.
[7.] Rafieizonooz, M., Mirza, J., Salim, M.R., Hussin, M.W. and Khankhaje, E. Investigation of coal bottom ash and fly ash in concrete as replacement for sand and cement. *Constr Build Mater*. 2016, 116, 15–24.
[8.] Asl, S.M.H., Javadian, H., Khavarpour, M., Belviso, C., Taghavi, M. and Maghsudi, M. Porous adsorbents derived from coal fly ash as cost-effective and environmentally-friendly sources of aluminosilicate for sequestration of aqueous and gaseous pollutants: A review. *J. Clean. Prod.*, 2019, 208, 1131–1147.
[9.] Ochedi, F.O., Liu, Y. and Hussain, A. A review on coal fly ash-based adsorbents for mercury and arsenic removal. *J. Clean. Prod.*, 2020, 267, 122143.
[10.] Rubel, A., Andrews, R., Gonzalez, R., Groppo, J., Robl, T. Adsorption of Hg and NOx on coal by-products. *Fuel*, 2005, 84, 911–916.
[11.] Mishra, M.K., Karanam, U.M.R. Geotechnical characterisation of fly ash composites for backfilling mine voids. *Geotech. Geol. Eng.*, 2006, 24, 1749–1765.
[12.] Peng, F., Liang, K.M., Hu, A.M. Nano-crystal glass–ceramics obtained from high alumina coal fly ash. *Fuel*, 2005, 84, 341–346.

[13.] Erol, M., Kucukbayrak, S., Ersoy-Mericboyu, A. Comparison of the properties of glass, glass–ceramic and ceramic materials produced from coal fly ash. *J. Hazard. Mater.*, 2008, 153, 418–425.
[14.] Pandey, V.C., Singh, N. Impact of fly ash incorporation in soil systems. *Agric Ecosyst Environ*, 2010, 136, 16–27.
[15.] Manoharan, V., Yunusa, I.A.M., Loganathan, P., Lawrie, R., Skilbeck, C.G., Burchett, M.D., Murray, B.R., Eamus, D. Assessments of class F fly ashes for amelioration of soil acidity and their influence on growth and uptake of Mo and Se by canola. *Fuel*, 2010, 89, 3498–3504.
[16.] Wang, S. Application of solid ash-based catalysts in heterogeneous catalysis. *Environ. Sci. Technol*, 2008, 42 (19), 7055–7063.
[17.] Na, J.G., Jeong, B.H., Chung, S.H., Kim, S.S. Pyrolysis of low-density polyethylene using synthetic catalysts produced from fly ash. *J. Mater. Cycles Waste Manag.*, 2006, 8, 126–132.
[18.] Mohan, S., Gandhimathi, R. Removal of heavy metal ions from municipal solid waste leachate using coal fly ash as an adsorbent. *J. Hazard. Mater.*, 2009, 169, 351–359.
[19.] Itskos, G., Koukouzas, N., Vasilatos, C., Megremi, I., Moutsatsou, A. Comparative uptake study of toxic elements from aqueous media by the different particle size-fractions of fly ash. *J. Hazard. Mater.*, 2010, 183, 787–792.
[20.] Sahoo, P.K., Kim, K., Powell, M.A., Equeenuddin, S.M. Recovery of metals and other beneficial products from coal fly ash: A sustainable approach for fly ash management. *Int. J. Coal Sci. Technol*, 2016, 3 (3), 267–283.
[21.] Matjie, R.H., Bunt, J.R., van Heerden, J.H.P. Extraction of alumina from coal fly ash generated from a selected low rank bituminous South African coal. *Miner. Eng.*, 2005, 18, 299–310.
[22.] Vadapalli, V.R.K., Klink, M.J., Etchebers, O., Petrik, L.F., Gitari, W., White, R.A., Key, D., Iwuoha, E. Neutralization of acid mine drainage using fly ash, and strength development of the resulting solid residues. *S. Afr. J. Sci.*, 2008, 104, 317–322.
[23.] Fan, M., Brown, R.C., Leeuwen, J.H.V., Nomura, M., Zhuang, Y. The kinetics of producing sulfate-based complex coagulant from fly ash. *Chem. Eng. Process*. 2003, 42, 1019–1025.
[24.] Nabi, B.G.R., Torabian, A., Ehsani, H., Razmkhah, N. Evaluation of industrial dyeing wastewater treatment with coagulants and polyelectrolyte as a coagulant aid. *Iran. j. environ. health sci. eng*. 2007, 4 (1), 29–36.
[25.] Semerjian, L., Ayoub, G.M. High-pH–magnesium coagulation–flocculation in wastewater treatment. *Adv. environ. Res*. 2003, 7 (2), 389–403.
[26.] Teringo, T. Magnesium hydroxide reduces sludge/improves filtering. *Pollut. Eng*. 1987, 19, 78–83.
[27.] Apua, M.C. Total dissolved solids and turbidity removal from acid mine drainage using a coal fly ash-based complex coagulant, *Int. j. adv. sci. eng. technol*. 2020, 8 (1), 51–55.
[28.] Barrett, J., Ewart, D.K., Hughes, M.N., Poole, R.K. Chemical and biological pathways in the bacterial oxidation of arsenopyrite. *FEMS Microbiol. Rev*. 1993, 11 (1–3), 57–62.
[29.] Stumm, W., Morgan, J.J. Aquatic Chemistry, 3rd ed. John Wiley and Sons, USA, 1996.
[30.] Langmuir, D. Aqueous environmental geochemistry, (No. 551.48 L3.), 1997.
[31.] Casas, J.M., Crisóstomo, G., Cifuentes, L. Speciation of the Fe (II)–Fe (III)–H_2SO_4–H_2O system at 25 and 50 °C. *Hydrometallurgy*. 2005, 80 (4), 254–264.
[32.] Yue, G., Zhao, L., Olvera, O.G., Asselin, E. Speciation of the H_2SO_4–$Fe_2(SO_4)_3$– $FeSO_4$–H_2O systemand development of an expression to predict the redox potential of the Fe^{3+}/Fe^{2+} couple up to 150 °C. *Hydrometallurgy*. 2014, 147–148, 196–209.
[33.] Rubisov, D.H. and Papangelakis, V.G. Sulphuric acid pressure leaching of laterites—speciation and prediction of metal solubilities “at temperature”. *Hydrometallurgy*. 2000, 58 (1), 13– 26.
[34.] Fan, M., Brown, R.C., Wheelock, T.D., Cooper, A.T., Nomura, M., Zhuang, Y. Production of a complex coagulant from fly ash. *Chem. Eng. J*. 2005, 106, 269–277.
[35.] Li, L., Fan, M., Brown, R.C., Koziel, J.A., Leeuwen, J. H. Production of a new wastewater treatment coagulant from fly ash with concomitant flue gas scrubbing. *J. Hazard. Mater*. 2009, 162, 1430–1437.
[36.] Kelmers, A.D., Egan, B.Z., Seeley, F.G., Campbell, G.D. Direct acid dissolution of aluminium and other metals from fly ash. *The Metallurgical Society of AIME, TMS paper A*. 1981, 81–24.
[37.] Matjie, R.H., Li, Z., Ward, C.R., French, D. Chemical composition of glass and crystalline phases in coarse coal gasification ash. *Fuel*. 2008, 87, 857–859.
[38.] Welham, N.J., Malatt, K.A., Vukcevic, S. The effect of solution speciation on iron–sulphur–arsenic–chloride systems at 298 K. *Hydrometallurgy*. 2000, 57 (3), 209–223.
[39.] Mazzocchitti, G., Giannopoulou, I., Panias, D. Silicon and aluminum removal from ilmenite concentrates by alkaline leaching. *Hydrometallurgy*. 2009, 96 (4), 327–332.
[40.] Babcan, J. Synthesis of jarosite $KFe_3(SO_4)_2(OH)_6$. *Geology*. Zb. 1971, 22 (2), 299–304.
[41.] Roeland, J., Dijkhuis, E. The minimisation of copper losses during iron and aluminium precipitation from zinc leach liquors. Technical University of Delft, The Netherlands, 2009.
[42.] Malenga, E.N., Mulaba-Bafubiandi, A.F., Nheta, W. Alkaline leaching of nickel bearing ammonium jarosite precipitate using KOH, NaOH and NH_4OH in the presence of EDTA and Na_2S. *Hydrometallurgy*. 2015, 155, 69–78.
[43.] Bellmann, F., Moser, B., Stark, J. Influence of sulfate solution concentration on the formation of gypsum in sulfate resistance test specimen. *Cem Concr Res*. 2006, 36, 358–363.